

Time-Resolved Studies of a Rolled-Up Semiconductor Microtube Laser

Ch. Strelow,^{1,*} M. Sauer,¹ S. Fehring,² T. Korn,² C. Schüller,²
A. Stemmann,¹ Ch. Heyn,¹ D. Heitmann,¹ and T. Kipp^{†1}

¹*Institut für Angewandte Physik und Zentrum für Mikrostrukturforschung,
Universität Hamburg, Jungiusstraße 11, 20355 Hamburg, Germany*

²*Institut für Experimentelle und Angewandte Physik,
Universität Regensburg, D-93040 Regensburg, Germany*

(Dated: August 14, 2018)

We report on lasing in rolled-up microtube resonators. Time-resolved studies on these semiconductor lasers containing GaAs quantum wells as optical gain material reveal particularly fast turn-on-times and short pulse emissions above the threshold. We observe a strong red-shift of the laser mode during the pulse emission which is compared to the time evolution of the charge-carrier density calculated by rate equations.

The most studied semiconductor microcavity lasers are micropillars^{1,2}, microdisks^{3,4} and photonic crystals^{5,6}. Their small size combined with high quality factors exhibits the possibility of low threshold lasing and single mode operation. Besides the pursuit of lowering the threshold also fast turn-on-times are desirable^{4,5}. Presently the fastest turn-on-times were achieved by using quantum wells (QWs) as gain material⁵ which have the disadvantage of high non-radiative recombination rates in the vicinity of the structured surfaces. To overcome this problem the surface can be passivated^{7,8}. Quantum dots offer a much lower surface recombination rate⁹ but have the disadvantage of a low carrier capture rate¹⁰ which lengthens the turn-on-time. In this work we present lasing in microtubes. These structures have the intrinsic advantage of nearly no unpassivated surfaces. Exploiting the self-rolling mechanism of thin strained semiconductor bilayers¹¹ we fabricated multi-walled microtubes that act as optical ring resonators¹². As optical gain medium we chose a GaAs QW. Applying sub-picosecond optical pumping we measured the time evolution of the photoluminescence (PL) emission at low temperature.

Our samples were grown by molecular beam epitaxy on (001) GaAs substrates. On top of a 40 nm AlAs sacrificial layer a 42 nm thick layer system is grown consisting of a 16 nm thick pseudomorphically strained barrier layer of $\text{In}_{0.16}\text{Al}_{0.30}\text{Ga}_{0.54}\text{As}$, a 4 nm GaAs QW, and a 22 nm $\text{Al}_{0.20}\text{Ga}_{0.80}\text{As}$ barrier. By selectively etching the sacrificial layer a predefined U-shaped mesa rolls up and forms a free-standing microtube bridge. Details of the fabrication are described in Refs. 12,13. The tube investigated in this work is shown in Fig. 1(a). It has a diameter of $5.74\ \mu\text{m}$ and 1.1 revolutions. In the free-standing part total internal reflection leads to waveguiding in the tube wall and to the formation of ring modes by constructive interference after a roundtrip¹². Very recently we showed

that a fully three-dimensional control of the eigenmodes can be achieved by the definition of lobes in the rolling edge¹⁴. In this work we used a different axial confinement mechanism. By etching two $t=4\ \text{nm}$ deep stripes of a distance $L_z=1.43\ \mu\text{m}$ before rolling-up we fabricated a rolled-up ridge waveguide, as shown schematically in Fig. 1(b). Here, it also becomes obvious that microtubes should have low surface recombination rates due to the nearly complete absence of gain material at the surface.

Our experiments were performed with a tunable Ti:Sa laser with 600 fs pulse length and 81 MHz repetition rate. The laser was focussed by a $40\times$ microscope objective ($\text{NA}=0.4$) onto the sample mounted in a continuous flow He cryostat at 4 K. The PL light is collected by the same objective, dispersed by a 25 cm spectrometer with 600 lines/mm grating and detected either by a streak camera (Hamamatsu Synchroscan) or a Si charge coupled device camera. The time resolution of the setup is 9 ps, measured from the FWHM of the pump laser. The excitation wavelength was set to 750 nm which excites only the QW and not the barriers, since the band gap of the InAlGaAs layer is increased by compressive strain inside the microtube structure. Figure 2 shows excitation power dependent measurements on our microtube. Emission spectra of the microtube for three different excitation powers (measured as time-averaged power of the pulsed laser) are shown in Fig. 2(b). The QW emits around 797 nm with a FWHM of about 4.5 nm. Its emission is modified by

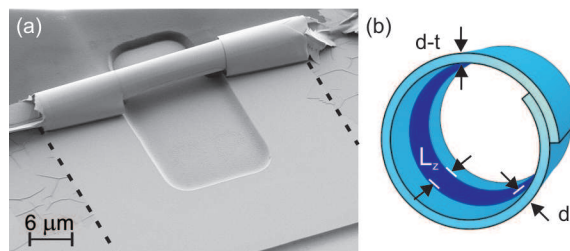


FIG. 1: (a) Scanning electron micrograph a microtube and its U-shaped mesa (dashed lines). (b) Unscaled sketch of the free-standing part of the tube.

[†]present address: Institut für Physikalische Chemie, Universität Hamburg, Grindelallee 117, 20146 Hamburg, Germany

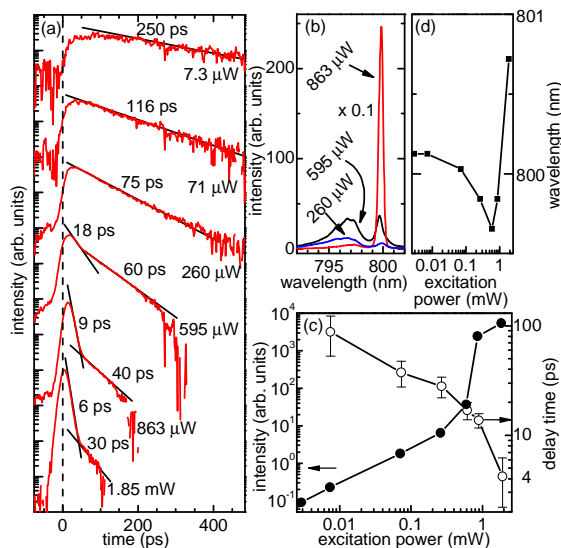


FIG. 2: Excitation power dependent measurements of the microtube in Fig. 1. (a) Time evolution of the emitted PL light. (b) PL spectra. (c) Time-integrated PL intensity and delay time between pump pulse and PL emission. (d) Wavelength of the lasing mode in the time-integrated spectra.

optical modes. We rule out strong-coupling effects since all estimated charge carrier densities exceed the saturation density for strong coupling¹⁵. The strong mode at 800 nm is an axial fundamental mode¹⁴ with one antinode in axial direction, determined from spatially resolved measurements (not shown). Figure 2(a) depicts the time evolution of the PL emission of the mode for different excitation powers. With increasing excitation power one clearly observes a shortening of the lifetime from 250 ps down to about 6 ps, determined by fitting the decay in a period longer than the time resolution (at least 20 ps) and calculating the $1/e$ lifetime. In addition we find a threshold behavior in the light-input/light-output (L-L) curve depicted in Fig. 2(c). Above a threshold between 260 μW and 59 μW the system starts lasing. With increasing excitation power more and more stimulated emission shortens the decay times and a short pulse appears at the onset of the PL emission. For 863 μW a single laser mode dominates the spectrum, as shown in Fig. 2(b). Interestingly, the decay times already shorten well below the threshold. We believe that between 7.3 μW and 71 μW population inversion is reached and amplified spontaneous emission shortens the decay time. The threshold power is quite high compared to values for microdisk lasers^{9,16} and photonic crystal laser^{5,10}. This is caused by the large surface to volume ratio of microtubes. In finite-difference time-domain simulations, assuming that only the quantum well absorbs power, we calculated that less than 2 % of the laser power are absorbed by the microtube. The threshold power might be much lower if one overcomes the difficulties of optical pumping, e.g., by electrical pumping.

Figure 2(c) depicts the delay between the arrival of

the pump pulse, determined by the stray light of the excitation laser, and the maximum of the PL emission. A clear drop of the turn-on-times with increasing excitation power is observed. For 863 μW we measured about 14 ps. By exciting with light linearly polarized perpendicular to the mode polarization^{12,13} and measuring in corresponding polarizations, turn-on-times even below the conventional time resolution can be determined. For 1.85 mW we find 4 ± 1.5 ps. Our turn-on-times are quite fast in comparison to values in Refs. 5,9, despite the absence of a fastened spontaneous decay rate by the Purcell effect. We attribute this to the nearly-resonant carrier excitation directly in the QW and the fast carrier relaxation in the QW. In addition we observed no relaxation oscillations in our experiments as often observed in microdisks^{4,9}. This is because microtubes have no charge-carrier reservoir like microdisks. In QW microdisk lasers diffusion from the middle part to the active region is a prerequisite in order to balance gain losses due to the very strong non-radiative surface state recombination.

Figure 2(d) shows the center wavelength of the time integrated lasing mode in dependence on the excitation power. Up to 595 μW we observe a strong blue shift followed by a strong red shift for higher excitation powers. The blue shift is caused by a change of the refractive index with an increasing charge carrier density for increasing excitation powers. Although untypical for pulsed measurements we attribute the red shift to heating which even destroys microtubes when excited with powers of typically 4 mW. Probably the thin microtube walls offer only a slow heat transfer to the substrate. A wavelength shift is also observed during the short PL emission and gives insight into the charge carrier dynamics on short time scales: Figure 3 (a) depicts false-color images taken by the streak camera at different excitation powers. Obviously, the lasing mode around 800 nm shifts to red during the emitted light pulse and the shift becomes larger for higher excitation powers. We fitted the spectral profiles at different times with Gaussians for the highest three excitation powers in Fig. 3(a). The results in form of amplitude, wavelength and width are depicted in Fig. 3(b)-(d). Interestingly, we also observe a dynamic change of the spectral width besides the red shift. The first photons emitted after excitation are emitted spontaneously and the line width reflects the cavity life time. Indeed, the width of 0.8 nm at the onset of PL emission is the same as measured well below the threshold in the time-integrated spectra. Then, the width decreases by 50% within about 20 ps, stays constant for 30 ps (when the maximum of the PL emission is reached) and again increases at the end of the PL pulse. We attribute this behavior to the dynamic change into the coherent light state, when the system lases, and back into the spontaneous emission regime when the lasing turns off. Line-width narrowing with increasing pump power is reported for other microlasers⁶, but here we observe it on the time scale.

To explain the time evolution of the emitted PL inten-

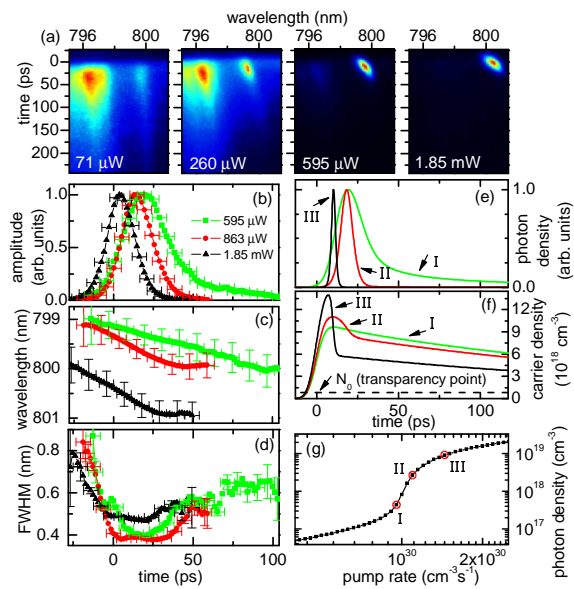


FIG. 3: (a) False-color images by the streak camera for different excitation powers. (b)-(d) Time evolution of the amplitude, wavelength and width of the lasing mode obtained by Gaussian fits at all times in (a). (e)-(g) Results for the time evolution of the photon density (e) and the charge carrier density (f) for three pump rates marked in the pump rate dependent photon density in (g) calculated by rate equations.

sity and the wavelength of the lasing mode we numerically solved rate equations for the charge-carrier density N and the photon density S :

$$\dot{N} = -\Gamma S G_0 (N - N_0) - \frac{N}{\tau_{sp}} + P(t), \quad (1)$$

$$\dot{S} = \Gamma S G_0 (N - N_0) + \beta \frac{N}{\tau_{sp}} - \frac{S}{\tau_p}. \quad (2)$$

Here, we assumed a constant differential gain of $G_0 = 5 \times 10^{-6} \text{ cm}^3/\text{s}$ and a value of $N_0 = 1.16 \times 10^{18} \text{ cm}^{-3}$ for N at the transparency point.⁴ For the optical confinement factor Γ we calculated 0.0563 and for the spontaneous emission factor β we assumed 0.01. According to the experiment we chose the spontaneous life time to $\tau_{sp} = 250 \text{ ps}$ [see Fig. 2(a) for low excitation power]. We neglected

non-radiative decays since for our comparative studies significant non-radiative decay rates do not change the results qualitatively. From the experimentally obtained cavity quality factor $Q = 1000$ we determined a photon lifetime τ_p in the cavity of 0.424 ps. The pump pulse we assumed to be Gaussian, i.e., $P(t) = P_0 e^{-(2t/w\sqrt{\ln 2})^2}$ with a FWHM of $w = 10 \text{ ps}$. The time-integrated photon density versus the pump rate is shown in Fig. 3 (g). A qualitative agreement to the experimental data in Fig. 2 (c) is observed. Figures 3 (e) and (f) depict the time evolution of S (normalized) and N for pump rates roughly corresponding to the excitation powers in the Fig. 3 (b)-(d). The calculated curve of S qualitatively reproduces the experimental data in Fig. 3(b). The time evolution of N can be compared to the time evolution of the wavelength in Fig. 3(c). N changes the refractive index linearly¹⁷ which on the other hand causes a linear shift of the mode wavelength. Consequently, the wavelength shift is a direct measure for N . Slightly above the threshold (pump rate I) N decays mainly spontaneously and thus exponentially. Well above the threshold (pump rates II, III) dominating stimulated emission leads to the observed fast drop of N . This behavior can directly be found in the measurements: At 595 μW (slightly above the threshold) the wavelength shift is slow and at 863 μW (well above the threshold) it changes from fast during the pulse emission to slow at its end. For 1.85 mW the shift does not become faster in contrast to the calculations. We believe that here the assumption of a constant gain breaks down. The mode might have shifted to different gain or the gain itself has changed e.g. due to saturation or renormalization effects or heating. The absolute values of the wavelength are generally not reproduced by the calculations. For high excitation powers heating leads to an additional red-shift of the laser mode.

In summary, we report on the demonstration of lasing in active microtube resonators. We observed fast turn-on times as compared to other micro-lasers and a characteristic red shift of the laser mode during pulsed emission. This behavior is reproduced by a rate equation model.

We acknowledge financial support by the Deutsche Forschungsgemeinschaft via SFB 508 and Graduiertenkolleg 1286 and 638.

* Electronic address: cstrelow@physnet.uni-hamburg.de

¹ M. Schwab, H. Kurtze, T. Auer, T. Berstermann, M. Bayer, J. Wiersig, N. Baer, C. Gies, F. Jahnke, and J. P. Reithmaier, Phys. Rev. B **74**, 045323 (2006).

² S. M. Ulrich, C. Gies, S. Ates, J. Wiersig, S. Reitzenstein, C. Hofmann, A. Löffler, A. Forchel, F. Jahnke, and P. Michler, Phys. Rev. Lett. **98**, 043906 (2007).

³ S. L. McCall, A. F. J. Levi, R. E. Slusher, S. J. Pearton, and R. A. Logan, Appl. Phys. Lett., 289 **60** (1992).

⁴ K. J. Luo, J. Y. Xu, H. Cao, Y. Ma, S. H. Chang, S. T. Ho, and G. S. Solomon, Appl. Phys. Lett. **77**, 2304 (2000).

⁵ H. Altug, D. Englund, and J. Vučković, Nature Physics **2**, 484 (2006).

⁶ S. Strauf, K. Hennessy, M. T. Rakher, Y.-S. Choi, A. Badolato, L. C. Andreani, E. L. Hu, P. M. Petroff, and D. Bouwmeester, Phys. Rev. Lett. **96**, 127404 (2006).

⁷ U. Mohideen, W. S. Hobson, S. J. Pearton, F. Ren, and R. E. Slusher, Appl. Phys. Lett. **64**, 1911 (1994).

⁸ D. Englund, H. Altug, and J. Vučković, Appl. Phys. Lett. **91**, 071124 (2007).

⁹ K. J. Luo, J. Y. Xu, H. Cao, S. H. Chang, S. T. Ho, and G. S. Solomon, Appl. Phys. Lett. **78**, 3397 (2001).

- ¹⁰ B. Ellis, I. Fushman, D. Englund, B. Zhang, Y. Yamamoto, and J. Vučković, *Appl. Phys. Lett.* **90**, 151102 (2007).
- ¹¹ V. Y. Prinz, V. A. Seleznev, A. K. Gutakovsky, A. V. Chehovskiy, V. V. Preobrazhenskii, M. A. Putyato, and T. A. Gavrilova, *Physica E* **6**, 828 (2000).
- ¹² T. Kipp, H. Welsch, Ch. Strelow, Ch. Heyn, and D. Heitmann, *Phys. Rev. Lett.* **96**, 77403 (2006).
- ¹³ Ch. Strelow, C. M. Schultz, H. Rehberg, H. Welsch, Ch. Heyn, D. Heitmann, and T. Kipp, *Phys. Rev. B* **76**, 045303 (2007).
- ¹⁴ Ch. Strelow, H. Rehberg, C. M. Schultz, H. Welsch, Ch. Heyn, D. Heitmann, and T. Kipp, *Phys. Rev. Lett.* **101**, 127403 (2008).
- ¹⁵ R. Houdré, J. L. Gibernon, P. Pellandini, R. P. Stanley, U. Oesterle, C. Weisbuch, J. O’Gorman, B. Roycroft, and M. Ilegems, *Phys. Rev. B* **52**, 7810 (1995).
- ¹⁶ V. Zwiller, S. Fälth, J. Persson, W. Seifert, L. Samuelson, and G. Björk, *J. Appl. Phys.* **93**, 2307 (2003).
- ¹⁷ J. G. Mendoza-Alvarez, F. D. Nunes, and N. B. Patel, *J. Appl. Phys.* **51**, 4365 (1980).